THE ASTROPHYSICAL JOURNAL, **258**:576–588, 1982 July 15


# EX HYDRAE: PHYSICAL PARAMETERS DERIVED FROM SIMULTANEOUS SPECTROSCOPY AND PHOTOMETRY

RONALD L. GILLILAND[1]
High Altitude Observatory, National Center for Atmospheric Research[2]
*Received 1981 October 15; accepted 1982 February 8*

## ABSTRACT

High time resolution spectrophotometry has been used to determine the orbital characteristics of the eclipsing dwarf nova system EX Hydrae. Simultaneous photometry and spectrophotometry show that the 67 min photometric period clearly appears spectroscopically as a modulation of emission-line intensities. Emission-line profiles are found to vary at one-half of the 67 min period as well as the orbital period. A new analysis of eclipse timings reveals a constant orbital period, while analysis of the 67 min variation reveals a significant period decrease. Models for the 67 min variation are discussed. The radial velocity half-amplitude of $K_1 = 58 \pm 9$ km s$^{-1}$, coupled with standard assumptions concerning the secondary component, suggests masses of $M_1 \sim 1.4\ M_\odot$ and $M_2 \sim 0.17\ M_\odot$ for the binary components.

*Subject headings:* stars: dwarf novae — stars: eclipsing binaries — stars: individual — X-rays: binaries

## I. INTRODUCTION

Although EX Hydrae was one of the first cataclysmic variables for which an accurate orbital period was obtained through photometric eclipse timings (Kraft and Krzeminski 1962), new properties of this interesting system continue to be discovered and have made interpretations of the system highly complex. EX Hya shows strong emission of hard and soft X-rays even during quiescence (Watson, Sherrington, and Jameson 1978; Córdova and Riegler 1979), a nearly unique property for the dwarf novae. Its stable photometric variation at $\sim 2/3$ the orbital period (hereafter referred to as $P_h \sim 67$ min, with the orbital period $P_o \sim 98$ min) is unique among the dwarf novae (Vogt, Krzeminski, and Sterken 1980, hereafter VKS). The 67 min period has also been detected in soft X-rays, although modulation in hard X-rays ($>2.4$ keV) is not evident (Heise 1981). EX Hya is also unusual in having infrequent outbursts ($\sim 4$ yr separation) of relatively low amplitude ($\sim 3$ mag), lasting only 2 days (Bateson 1981).

Due to its interesting photometric behavior, EX Hya has been extensively studied with high time resolution photometry (VKS and references therein). As one of the brighter cataclysmic variables ($B \approx 13.4$), EX Hya is also accessible to spectroscopic analysis with both high temporal and spectral resolution. Kraft (1964) described the essential spectral features: broad and doubled hydrogen emission, weaker He I and II emission, and an "S wave" component as found earlier in the eclipsing system WZ Sge. Only recently have additional spectroscopic results been published. Breysacher and Vogt (1980, hereafter BV) obtained 19 spectrograms in 1976 April with the ESO 1.52 m telescope, derived orbital parameters, and found a correlation of emission line strengths with $P_h$. Cowley, Hutchings, and Crampton (1981, hereafter CHC) obtained 16 spectrograms in 1980 February with the CTIO 4 m telescope. CHC also derived orbital parameters and investigated possible correlations of line intensities with $P_h$. The derived velocity amplitudes of BV and CHC differ by 32%, derived masses of the primary component by a factor of 2, and contrary conclusions are reached concerning the variability of emission-line strengths.

The results of BV are rather marginal due to their limited spectral and time resolution—typical exposures were $\sim 0.15\ P_o$ or $\sim 0.22\ P_h$. Therefore, the observations discussed below (obtained in 1980 March with the CTIO 4 m and CTIO 60 cm telescopes) were initiated in order to test, or extend, the results obtained by BV concerning the radial velocity curve and line intensity variations with $P_h$. The results of this paper are in essential agreement concerning both the radial velocities and line intensity variations with the work of BV.

The spectroscopic and photometric results presented here should be of use, in conjunction with previous photometric and X-ray results, in helping to discriminate between the various models presented for EX Hya.

[1]Visiting Astronomer, Cerro Tololo Inter-American Observatory, supported by the National Science Foundation under contract No. 78-27879.

[2]The National Center for Atmospheric Research is sponsored by the National Science Foundation.

## II. SPECTROSCOPIC DATA

Spectra were obtained using the SIT vidicon with the Ritchey-Chrétien spectrograph on the 4 m CTIO telescope in 1980 March. A dispersion of 0.95 Å per channel was used with the vidicon resulting in 2–3 Å resolution. Most exposure times were 4 min yielding ~17 spectra over an orbital cycle or ~12 spectra per 67 min cycle. At the above dispersion about 450 Å of useful spectral coverage was obtained. In Table 1 we present a journal of the observations which were obtained in two wavelength regions centered at ~4200 Å (Hγ and Hδ) and ~4700 Å (Hβ and He II λ4686). At the region covering Hγ and Hδ 29 consecutive scans were obtained covering two full orbital cycles. At the region covering He II λ4686 and Hβ 17 consecutive scans were taken covering one full orbital cycle, with an additional six scans obtained less than one hour later. Figure 1 shows typical 4 min scans for both wavelength regions.

Simultaneous photometry was obtained with a photon counting system on the 60 cm telescope of CTIO and will be discussed extensively in a later section.

## III. RADIAL VELOCITY CURVE

As discussed more extensively in an earlier paper (Gilliland 1982) radial velocities were obtained by fitting a Lorentzian profile to the wings of the Balmer lines. The central points within $\pm 1000$ km s$^{-1}$ (1 Å $\approx 70$ km s$^{-1}$) were assigned a weight of zero. The fitting was extended to $\pm 3000$ km s$^{-1}$ from line center. The radial velocities are not sensitive to small variations of the number of excluded central points, but could be sensitive to excluding significantly fewer central points. (The line profile variations tend to be restricted to the central portions of the line profile; further discussion below.) Velocities for the He II λ4686 line, which does not show a doubled profile, were obtained by fitting the whole line within $\pm 3000$ km s$^{-1}$ of the line center. The derived radial velocities for Hγ, Hδ, Hβ, and He II λ4686 are included in Table 1.

The resulting orbital parameters obtained from fitting the radial velocities of each line separately are given in Table 2. The adopted radial velocity half-amplitude of $58 \pm 9$ km s$^{-1}$ results from a simultaneous fit to all four lines from a total of 52 spectral scans. The radial velocities and best fit orbital solution ($\varepsilon = \omega = 0$ assumed) are shown in Figure 2.

Since EX Hya shows grazing eclipses of the hot spot, the inclination angle can be fixed fairly precisely at $i = 75 \pm 10°$ (BV). The system parameters derived using this inclination are summarized in Table 3. In addition, several other limits can be placed on the mass of the primary. A lower limit to the mass of the primary can be set from a measurement of the half-width at zero intensity of the emission lines and the assumption that the line broadening is due to Keplerian velocities in a disk. Using Shipman's (1977) calibration of the mass–radius relation for white dwarfs and the highest observed line widths (~4000 km s$^{-1}$; see Fig. 3 which shows mean profiles), we find $M_1 > 0.8\ M_\odot$. The assumption that the secondary is a lower main-sequence star filling its Roche lobe (Robinson 1976; Warner 1976) leads to the mass estimate $M_2 = 0.17\ M_\odot$ (BV and CHC). Using the derived mass function and assuming $i \approx 75°$, $M_2 = 0.17\ M_\odot$, we find $M_1 \approx 1.6\ M_\odot$ with large potential error. Thus the lower limit for $M_1$ based on line widths is a rather mild constraint on the solution. Clearly if the primary is a white dwarf, the Chandrasekhar limit demands that an upper limit on $M_1$ be taken resulting in $M_1 \lesssim 1.4\ M_\odot$.

The derivation of reliable radial velocities is a difficult problem for the cataclysmic variables because line profile changes as a function of orbital phase are known to occur. In particular the "S wave" component which is thought to arise from either the gas stream or hot spot leads to a large change of the relative heights of the double emission peaks at the orbital cycle (e.g., see Fig. 6). Clearly changes of $V/R$ alter the centroid of the total emission line and may significantly influence the derived radial velocities depending upon measurement techniques. The standard approach (used here and by BV, CHC) is to assume that line profile changes are restricted to the central regions of the doubled emission line; thus, measuring positions of the line wings is assumed to provide radial velocities free of errors induced by line profile changes. We have been able to test the hypothesis that the line wings provide radial velocities independent of line profile (taken as $V/R$) changes due to two circumstances: (1) We obtain velocities by fitting a Lorentzian profile to the emission lines (digital intensity data) with a nonlinear least squares routine. Specific portions of the line core can be assigned zero weight, thus testing for consistency of different definitions of the line wing. (2) EX Hya fortuitously provides a means of testing for effects in the radial velocities due to $V/R$ changes because it shows a $V/R$ variation at a period different from the orbital period. As discussed at length in § V, EX Hya shows a significant $V/R$ variation at a period of 33.6 minutes.

We have analyzed the radial velocities of Hδ and Hγ with three different definitions of the line core. The separate line analyses using $\pm 1000$ km s$^{-1}$ from line center are presented in Table 2—a combined fit to Hδ + Hγ yields $K_1 = 53.5 \pm 8.9$ km s$^{-1}$. Using $\pm 1200$ km s$^{-1}$ as the line core yields $K_1 = 65.0 \pm 9.9$ km s$^{-1}$, while $\pm 1400$ km s$^{-1}$ yields $K_1 = 55.6 \pm 9.2$ km s$^{-1}$. The mean for the above three trials is $K_1 = 58.0 \pm 9.3$ km s$^{-1}$, the same as the overall adopted mean. The scatter of velocities increases slightly as more central points are excluded from the fit. The radial velocity residuals from the cosine fit at $P_0$ were checked for periodicity at $P = 33.6$ min as might be induced by line profile changes.

TABLE 1

SPECTROSCOPIC OBSERVATIONS OF EX HYDRAE

| Epoch(ET)[a] 2,444,320.+ | $\phi_o$ | $\phi_h$ | Velocity[b] Hγ/Hβ (km s$^{-1}$) | Velocity Hδ/He II (km s$^{-1}$) | Equiv. Width 0.6Hγ+0.4Hδ He II | V/R Hγ/Hβ |
|---|---|---|---|---|---|---|
| 2.7240 | 0.084 | 0.559 | −62.8 | −44.6 | 40.90 | 0.93 |
| 2.7301 | 0.174 | 0.691 | +11.5 | −39.4 | 49.25 | 0.79 |
| 2.7368 | 0.272 | 0.834 | −44.8 | −53.6 | 54.91 | 0.90 |
| 2.7434 | 0.369 | 0.977 | −45.2 | −30.1 | 54.82 | 0.97 |
| 2.7495 | 0.458 | 0.107 | −11.2 | +5.2 | 50.19 | 1.01 |
| 2.7545 | 0.531 | 0.215 | +1.5 | +16.0 | 45.38 | 1.04 |
| 2.7592 | 0.600 | 0.316 | +64.2 | +45.5 | 37.96 | 0.98 |
| 2.7639 | 0.669 | 0.417 | +34.1 | +36.3 | 35.22 | 1.12 |
| 2.7684 | 0.734 | 0.512 | +27.8 | +7.7 | 36.78 | 1.21 |
| 2.7728 | 0.800 | 0.608 | +33.9 | +71.1 | 43.56 | 1.02 |
| 2.7776 | 0.870 | 0.712 | +33.3 | +36.3 | 50.15 | 0.97 |
| 2.7821 | 0.935 | 0.807 | +35.1 | +32.3 | 55.04 | 0.96 |
| 2.7867 | 0.003 | 0.907 | −34.9 | −0.2 | 59.29 | 0.89 |
| 2.7912 | 0.069 | 0.003 | −31.2 | −17.4 | 56.41 | 0.98 |
| 2.7956 | 0.134 | 0.098 | −8.9 | +8.6 | 51.56 | 0.90 |
| 2.8001 | 0.199 | 0.193 | −59.2 | −64.0 | 49.71 | 0.87 |
| 2.8053 | 0.276 | 0.306 | −28.4 | −79.7 | 45.17 | 0.83 |
| 2.8101 | 0.346 | 0.408 | −25.7 | −42.8 | 38.97 | 0.99 |
| 2.8145 | 0.411 | 0.504 | −31.5 | −43.2 | 39.49 | 1.06 |
| 2.8196 | 0.486 | 0.614 | −65.6 | −3.1 | 46.56 | 1.08 |
| 2.8241 | 0.551 | 0.709 | +12.0 | +14.3 | 50.71 | 1.01 |
| 2.8286 | 0.618 | 0.807 | +18.6 | +33.2 | 57.67 | 1.03 |
| 2.8332 | 0.684 | 0.905 | +70.9 | +119.0 | 54.80 | 1.05 |
| 2.8383 | 0.759 | 0.014 | +73.4 | +74.1 | 50.42 | 1.05 |
| 2.8427 | 0.824 | 0.109 | +49.1 | +89.9 | 44.04 | 1.07 |
| 2.8471 | 0.889 | 0.204 | +16.8 | +36.7 | 42.17 | 0.97 |
| 2.8515 | 0.953 | 0.299 | +53.5 | +5.6 | 38.04 | 0.90 |
| 2.8563 | 0.023 | 0.401 | −14.8 | +18.1 | 43.60 | 0.89 |
| 2.8606 | 0.087 | 0.495 | −20.9 | −30.2 | 44.03 | 0.88 |
| 4.6948 | 0.967 | 0.899 | +66.7 | +27.3 | 10.25 | 0.86 |
| 4.6997 | 0.039 | 0.006 | −55.6 | −6.2 | 9.68 | 1.04 |
| 4.7043 | 0.106 | 0.104 | −29.4 | +83.0 | 8.06 | 0.97 |
| 4.7086 | 0.169 | 0.195 | −44.7 | −106.0 | 8.33 | 0.94 |
| 4.7128 | 0.232 | 0.287 | −96.5 | −133.0 | 9.82 | 0.90 |
| 4.7171 | 0.294 | 0.379 | −55.8 | +144.0 | 7.95 | 0.87 |
| 4.7214 | 0.357 | 0.471 | −36.7 | −59.2 | 7.03 | 0.92 |
| 4.7256 | 0.419 | 0.562 | −13.9 | +50.0 | 7.20 | 1.01 |
| 4.7299 | 0.482 | 0.654 | −60.2 | −108.0 | 8.71 | 1.03 |
| 4.7342 | 0.544 | 0.745 | −44.8 | −134.0 | 8.62 | 1.05 |
| 4.7384 | 0.606 | 0.837 | +31.4 | +82.9 | 8.93 | 1.04 |
| 4.7427 | 0.669 | 0.928 | +51.2 | +89.8 | 9.69 | 1.05 |
| 4.7470 | 0.732 | 0.021 | +47.9 | +94.3 | 8.27 | 1.07 |
| 4.7513 | 0.795 | 0.113 | +62.2 | +25.5 | 9.67 | 1.08 |
| 4.7556 | 0.858 | 0.206 | +46.2 | +60.0 | 8.80 | 1.02 |
| 4.7599 | 0.921 | 0.298 | +61.7 | −74.0 | 8.91 | 0.97 |
| 4.7641 | 0.983 | 0.389 | +39.1 | +40.5 | 7.77 | 0.89 |
| 4.8401 | 0.097 | 0.022 | −55.8 | +21.6 | 10.89 | 0.95 |
| 4.8444 | 0.159 | 0.113 | −92.8 | −80.0 | 10.09 | 0.94 |
| 4.8487 | 0.222 | 0.205 | −77.3 | −0.6 | 8.58 | 0.84 |
| 4.8529 | 0.284 | 0.297 | −66.3 | +133.2 | 9.03 | 0.86 |
| 4.8572 | 0.347 | 0.388 | −85.3 | +8.1 | 8.52 | 0.85 |
| 4.8615 | 0.410 | 0.480 | −100.5 | −114.8 | 7.46 | 1.01 |

[a] Epochs and phases are for time of mid-exposure. All scans are 4 min integrations except for the first four scans (6 min) and the following scan (5 min).

[b] Zero points of 33.2, −8.0, −35.6, and 30.5 km s$^{-1}$ have been removed from the Hγ, Hβ, Hδ, and He II, velocities, respectively.

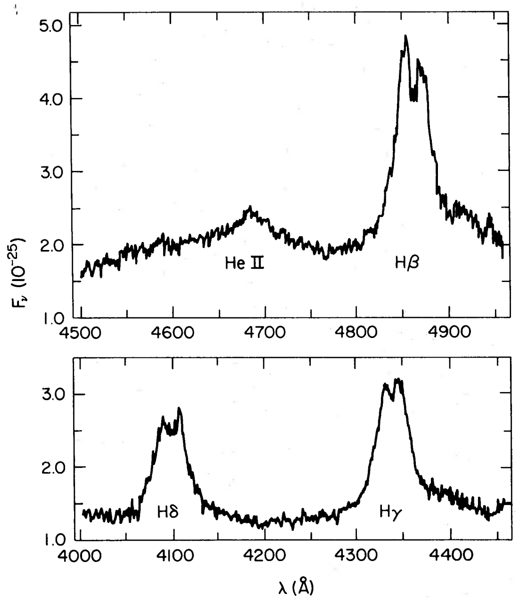


FIG. 1.—Absolute flux ($F_\nu$) in ergs cm$^{-2}$ s$^{-1}$ Hz$^{-1}$ plotted vs. wavelength. The upper panel shows a typical 4 min integration (epoch of midscan at 4.8437; see Table 1) at the He II λ4686, Hβ spectral region. A typical scan (epoch 2.7912) for the Hδ, Hγ region is shown in the lower panel.

TABLE 2

RADIAL VELOCITY FITS EX HYDRAE

| Line | $K_1$ (km s$^{-1}$) | γ (km s$^{-1}$) | $\sigma_{SD}$ (km s$^{-1}$) | $\phi_o$ (maximum) |
|---|---|---|---|---|
| Hδ | 59.8±12.1 | −30.6 | 23.0 | 0.76 |
| Hγ | 47.2±13.3 | +32.6 | 25.3 | 0.76 |
| Hβ | 71.6±16.0 | −20.2 | 27.2 | 0.79 |
| He II λ4686 | 59.7±40.7 | −25.1 | 66.0 | 0.78 |
| All lines | 57.7±8.7 | −9.3±35.0 | 27.7 | 0.77 |

TABLE 3

EX HYDRAE ORBITAL PARAMETERS[a]

| Parameter | Units | Value |
|---|---|---|
| $T_0$ ........... | ET | 2437699.9419±2 |
| $P$ ............ | days | 0.068233838±3 |
| $K_1$ ........... | km s$^{-1}$ | 58±9 |
| γ ............ | km s$^{-1}$ | −9±35 |
| $a \sin i$ ........ | km | $5.4\pm1.0\times10^4$ |
| $f(M)$ ......... | $M_\odot$ | $1.4\pm0.9\times10^{-3}$ |
| $i$ ............. | degrees | 75±10 |
| $M_1$ ........... | $M_\odot$ | 1.4±0.2 |
| $M_2$ ........... | $M_\odot$ | 0.17±0.05 |

[a]We have assumed $\varepsilon = \omega = 0$.

The results in order of low to high line core definitions are $K = 6.3\pm8.3$, $1.8\pm9.9$, $3.4\pm9.0$ km s$^{-1}$ with phase shifts of −0.41, −0.23, −0.34 relative to the $V/R$ variation. In no case is there a significant velocity effect induced by the $V/R$ variation, although at the smallest core definition a suggestion of an inverse correlation is present as would be expected physically. $V/R$ positive will shift the line centroid toward the blue, thus yielding too small a velocity near $\phi_o = 0.75$, the approximate orbital phase of maxima for both $V/R$ and $K_1$. Therefore the most likely effect of $V/R$ orbital variations will be to yield too small a $K_1$ estimate. From the above results we can not rule out a small effect, but under the assumption that the $V/R$ variations at the two periods influence the radial velocity determinations in the same linear form, any such effect at $P_o$ must be less than the errors quoted in Table 2.

## IV. PHOTOMETRY

We obtained photometric observations of EX Hya over parts of four nights in white light with a single

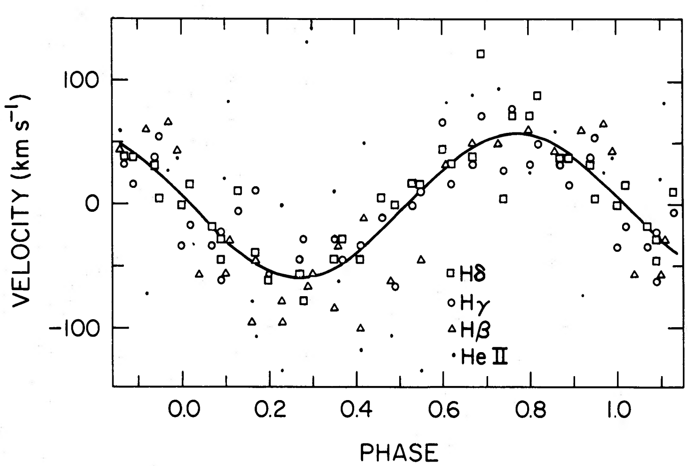


FIG. 2.—Radial velocity curve for EX Hya. Gamma velocities have been taken out for each line separately (see Table 2). Phase is with respect to the linear eclipse ephemeris derived in this paper. Weights for the two He II λ4686 velocities near phase 0.3 have been set to zero in the least squares fit. The continuous curve represents a fit to all four lines simultaneously with relative weights inversely proportional to $\sigma_{SD}^2$ for the individual determinations (see Table 2).

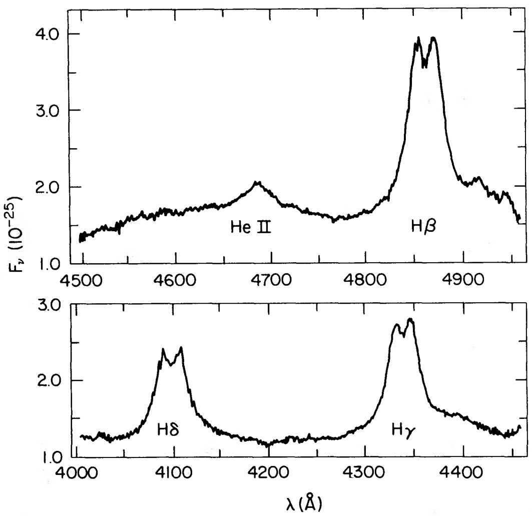


FIG. 3.—Absolute flux ($F_\nu$) in ergs $cm^{-2}$ $s^{-1}$ $Hz^{-1}$ plotted vs. wavelength. Upper panel is an average over the first 17 four minute scans at He II and Hβ covering about 1.2 orbital cycles. The lower panel is an average over all 29 scans at Hδ and Hγ covering two full orbital cycles and representing 125 minutes of integration.

channel photometer on the CTIO 60 cm telescope. Short (1–2 hour) runs were obtained on March 21 and 22 to determine new epochs for both the 67 min cycle and eclipses. On March 23 a continuous 6 hour run with 30 s integrations was obtained to allow simultaneous spectroscopic and photometric observations. On March 25 a nearly continuous 5 hour run with 15 s integrations was also obtained covering the same time as the 4 m spectroscopy. Sky and comparison observations were typically obtained at half-hour intervals. Short interruptions were made at ~10 minute intervals to check the centering, since offset guiding was not available. Figure 4 shows the photometric observations for March 23 and 25. The photometric observations are used to: (1) derive new ephemerides for the 67 min and orbital variations, (2) search for periodicities—particularly at the 40 min harmonic of the 67 min and orbital cycles, (3) facilitate a proper discussion of line property variations compared to the 67 min cycle (see § V).

The photometry obtained in 1980 March allows for a 28% extension of the baselines used by VKS to determine ephemerides for the 67 min and orbital cycles. In Table 4 we list 10 moments of maxima for the 67 min cycle determined in this study and include six additional moments from Warner and McGraw (1981). All referenced times in this paper are in ephemeris time, the correction to HJD for 1980 March being +0.0006 days. Also in Table 4 are 10 moments of minima for the eclipse cycle from this study and four additional moments from Warner and McGraw. In Table 5 the new ephemerides (fitting moments from VKS, corrected to ephemeris time, and Table 4 of this paper), assuming both linear and quadratic fits, are shown for the two cycles. Figure 5 shows $O-C$ versus cycle number for the 67 min variation with respect to the VKS ephemeris and the orbital cycle with respect to the Mumford (1967) linear ephemeris. With respect to the ephemerides of VKS the 1980 timings show a mean $O-C$ of $+0.0010 \pm 0.0005$ days for the eclipse minima and $-0.009 \pm 0.001$ days for the photometric maxima at 67 min. Both of these deviations lead to completely new interpretations of possible period changes. The quadratic term for the eclipses is now totally insignificant (VKS claimed significance at the 3 σ level). The ephemeris for the 67 min cycle did not show a significant quadratic term in the VKS analysis, but shows a highly significant quadratic term in our analysis.

Our 1980 March eclipse timings exhibit a systematic positive $O-C$ deviation from the ephemeris of Table 5 by ~0.0005 days. The 1976 April eclipse timings of both VKS and Warner and McGraw (1981) exhibit a systematic negative $O-C$ deviation from the new ephemeris of ~ −0.0005 days. Warner and McGraw note that EX Hya was near the bright end of its 13.7–12.7 mag range during their observing run. They suggest that near maximum brightness the accretion disk is somewhat extended leading to an earlier formation of the hot spot. In our case differential photometry with comparison star g of Warner (1977) yielded the following magnitudes for EX Hya: at ET(2,444,320.6347) $V=13.43$, $B-V=0.05$, $U-B=-1.23$; at ET(2,444,321.8059) $V=13.35$, phase of the 67 min cycle being 0.69 and 0.85 for the two epochs, respectively. Thus EX Hya was near minimum light in 1980 March—consistent with a smaller accretion disk, positive $O-C$, and sharp eclipse bottoms. Our observations support the contention of Warner and McGraw that the scatter of eclipse timings in Figure 5 could be reduced by taking into account the correlation between system brightness and $O-C$ timings.

At this point an aside is in order to discuss the statistical significance and probable error determinations for ephemeris coefficients. Pringle (1975) has given a discussion of statistical significance for the quadratic term under the assumption that the data points are distributed around the fitted curve in a Gaussian fashion. VKS used the significance test provided by Pringle, as well as the redundant error estimate on individual coefficients of a linear least squares analysis (see, e.g., Bevington 1969)—both estimates agreeing at significance of the quadratic term for eclipses of EX Hya exceeding 99%. However, as noted by Warner and McGraw (1981), the eclipse timings for EX Hya often differ in a systematic sense from predicted times for a given night or observing run. Such systematic deviations may result from physical variations within the system. The individual eclipse moments thus do not show a Gaussian distribution about the fitted curve. The signifi-

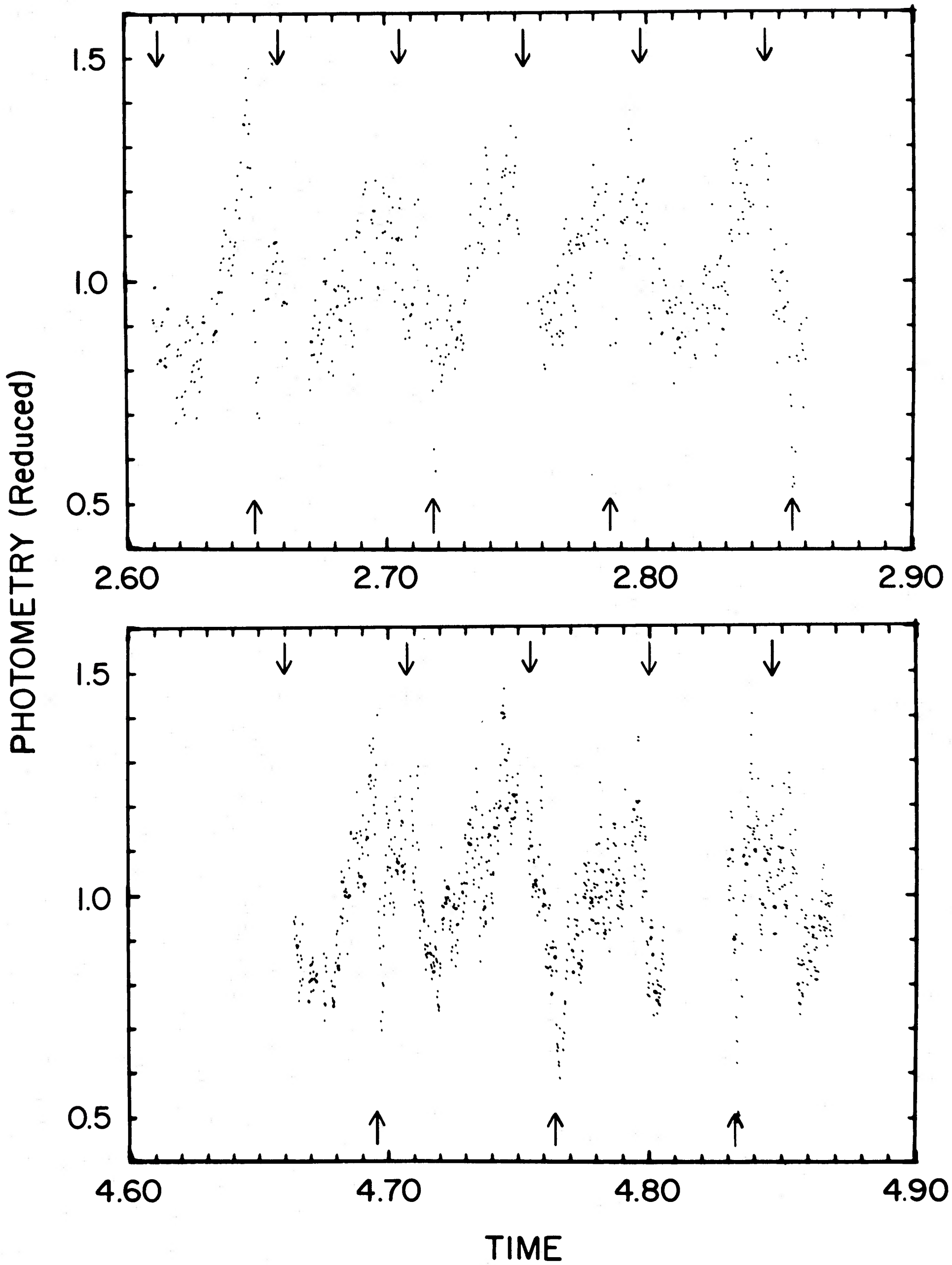


FIG. 4.—Photometry from 1980 March 23 in the upper panel (30 s integrations normalized by 77272). Lower panel shows 61 cm photometry from 1980 March 25 (15 s integrations normalized by 39023). Both runs have been sky subtracted and corrected for variable extinction. Times are ET (2,444,320.+). Downward and upward pointing arrows represent predicted times for the 67 min maxima and eclipse minima respectively from VKS.

cant autocorrelation of $O-C$ times during a given night or observing run effectively reduces the number of degrees of freedom used for the error estimate. The number of degrees of freedom should be reduced by a factor of about 2 (assuming autocorrelation within a single night) to about 5 (assuming autocorrelation throughout a three–four night observing run). We have adopted arbitrarily a factor of 3 reduction in degrees of freedom for error estimates of the EX Hya orbital ephemeris. (For systems such as Z Cha, OY Car, and HT Cas, which show eclipses of the central object, a correction as outlined above should not be necessary.) With this adjustment the quadratic term derived by VKS is no longer significant ($\sigma$ is inversely proportional to the

TABLE 4

PHOTOMETRIC MOMENTS[a]

| Eclipses (ET 2,400,000.+) | 67 min Maxima (ET 2,400,000.+) |
|---|---|
| 42872.4071 | 42872.361 |
| 42872.4754 | 42872.403 |
| 42872.5435 | 42872.457 |
| 42872.6118 | 42872.498 |
| | 42872.548 |
| 44320.8760 | 42872.598 |
| 44321.8985 | 44320.832 |
| 44322.6508 | 44322.647 |
| 44322.7189 | 44322.700 |
| 44322.7870 | 44322.745 |
| 44322.8551 | 44322.790 |
| 44324.6976 | 44322.838 |
| 44324.7658 | 44324.700 |
| 44324.8338 | 44324.745 |
| | 44324.792 |
| | 44324.840 |

[a]Epochs 42000+ are from Warner and McGraw (1981); 44000+ are from this study.

degrees of freedom) and the discrepancies with this study are obviated. Error estimates for binary star ephemerides should in general be regarded as lower limits due to the possibility of non-Gaussian error distributions.

Since the random errors in estimating times of maxima for the 67 min cycle are much larger than any systematic errors due to physical changes in the accretion disk, it is not necessary to alter the standard error estimate. The quadratic term for the 67 min ephemeris is significant at well above the 99% level. From the elements given in Table 5 we may derive a time scale (Pringle 1975) for the observed period change of $P/\dot{P} = -2.8 \times 10^6$ years. Since the eclipse minima do not show a change of period ($P/\dot{P}$ as small as $10^7$ years for the orbit can be excluded at the 5 $\sigma$ level of significance), the change of period for the 67 min variation is important in considering possible models (discussed later). Although the formal significance of the 67 min period change is high, we urge caution in interpreting possible causes until confirmation of the change over a longer time base is attained.

Warner and McGraw (1981) have suggested that EX Hya may be an intermediate polar in which beamed emission from a white dwarf rotating at 40 min interacts with the orbital period to yield a 67 min cycle. We have analyzed the two long, continuous photometry runs for evidence of periodicities. The 67 min cycle explains some 45% of the variance (peak to peak variation of 0.30 magnitudes) in these two runs (in all cases points within 2 min of eclipse were omitted from the analysis). A smaller variation near half the orbital cycle explains ~5% of the variance in the combined data sets—this may be related to a possible variation at $\frac{1}{2}P_o$ suggested by Mumford (1967), although more extensive data sets need to be examined to prove its reality. This suggests the presence of a slight bimodal flux inhomogeneity in the accretion disk. (The variation seems to be at a few percent less than $\frac{1}{2}P_o$, although the data are insufficient to adequately determine the period.) Evidence for a variation near 40 min was conspicuously absent from analyses of the two data sets taken either separately or combined. Any coherent white light variation near the sought-after 39.85 min rotation period must have been at an amplitude fitting less than 0.5% of the variance—two orders of magnitude smaller than the 67 min variation.

## V. LINE PROFILE, EQUIVALENT WIDTHS, AND CONTINUUM VARIATIONS

In order to study further the nature of the 67 min variation we have examined modulations of $V/R$, the ratio of the violet and red emission peaks of individual lines, and equivalent widths as functions of both the orbital ($\phi_o$) and hump ($\phi_h$) phases. $V/R$ serves primarily as a measure of line asymmetry caused by azimuthal variations in the disk, e.g., the "S wave" introduced by the hot spot. Equivalent width variations, in conjunction with continuum intensities from the spectrophotometry

TABLE 5

EX HYDRAE EPHEMERIDES[a]

| Cycle | $T_o$ (ET 2,400,000.+) | $P$ (days) | $\gamma$ (days) | $\sigma_{SD}$ (days) |
|---|---|---|---|---|
| 67 min ... | 37699.8920±6 | 0.046546420±7 | | 0.0037 |
| 67 min ... | 37699.8900±6 | 0.046546549±20 | $-1.05 \pm 0.16 \times 10^{-12}$ | 0.0032 |
| Orbital ... | 37699.9419±2 | 0.068233838±3 | | 0.0004 |
| Orbital ... | 37699.9419±2 | 0.068233837±10 | $1.3 \pm 12.5 \times 10^{-14}$ | 0.0004 |

[a]Ephemeris equation is ET(epoch) $= T_o + PE + \gamma E^2$, where $E$ is the cycle count after $T_o$. As noted in the text the quoted errors for the orbital cycle assume a factor of 3 reduction in effective degrees of freedom. A total of 140 data points entered the calculation for the 67 min cycle, with 151 data points determining the orbital ephemeris.

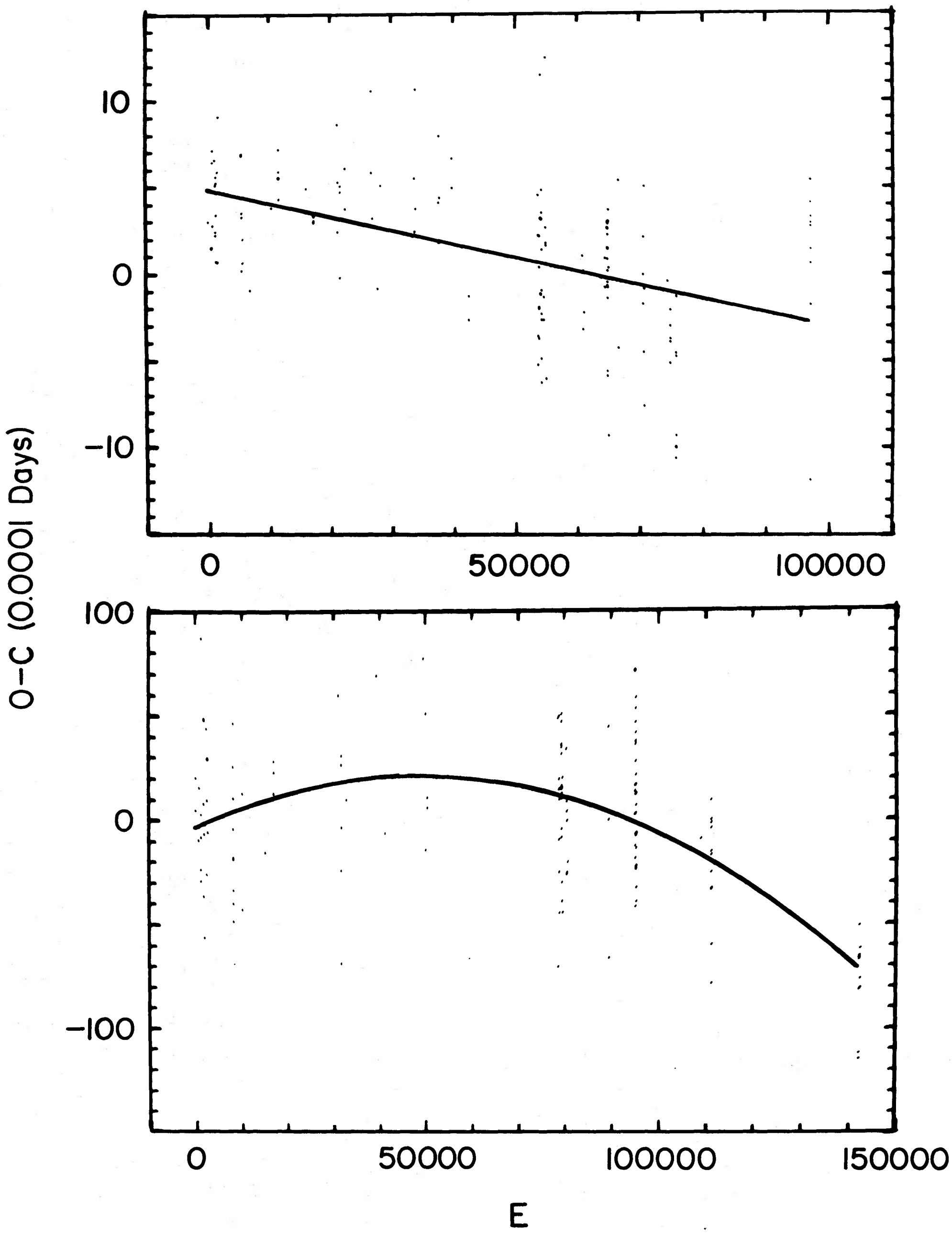


FIG. 5.—$O-C$ residuals vs. cycle number $E$ for the eclipse minima with respect to Mumford's (1967) linear ephemeris, solid line is best linear fit (*upper panel*). Lower panel shows $O-C$ residuals for the 67 min photometric maxima with respect to the linear ephemeris of VKS, the solid curve is the best fit parabola. Units for both diagrams are 0.0001 days.

and the simultaneous white light photometry discussed in § IV, yield firm measures of line intensity changes. Table 1 contains data for the 52 spectral scans discussed above, including phases of mid-exposure with respect to the orbital and hump ephemerides of this paper, equivalent widths, and $V/R$ ratios for selected lines.

In Figure 6 $V/R$ ratios for H$\delta$, H$\gamma$, and H$\beta$ are shown plotted against $\phi_o$. Clearly $V/R$ is a function of the orbital phase. The orbital component of $V/R$ accounts for 62% of the total variance. Phased cosine fits to the $V/R$ data are summarized in Table 6. The orbital variation of $V/R$ can be explained via the standard "S wave" model in which the mass transfer stream intersects the accretion disk slightly ahead of the line of centers creating a hot spot. The peak violet to red emission ratio occurs at $\phi_o = 0.66$, which is consistent

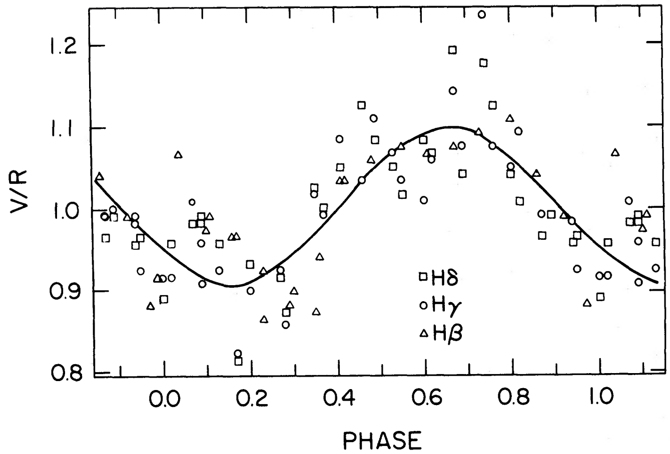


FIG. 6.—$V/R$ (ratio of violet to red emission component heights) vs. the orbital phase (ephemeris from this paper) for Hδ, Hγ, and Hβ. Solid line is best fit cosine curve.

TABLE 6
EQUIVALENT WIDTH AND PROFILE ANALYSES

| Line | Cycle | Quantity | Zero Point | Half-amp. | $\sigma_{SD}$ | $\phi_{max}$ |
|---|---|---|---|---|---|---|
| Hδ ............... | 67 min | EW | 38.29 | 7.42 | 2.56 | 0.91 |
| Hγ ............... | 67 min | EW | 53.56 | 9.61 | 3.33 | 0.90 |
| Hγ ............... | Orbital | EW | 53.20 | 1.91 | 7.77 | |
| Hβ ............... | 67 min | EW | 55.29 | 9.21 | 5.51 | 0.92 |
| He II λ4686 ....... | 67 min | EW | 8.66 | 0.90 | 0.72 | 0.02 |
| Hδ+Hγ+Hβ ... | 67 min | EW | 1.000 | 0.181 | 0.08 | 0.91 |
| Hδ ............... | Orbital | $V/R$ | 0.986 | 0.09 | 0.05 | 0.64 |
| Hγ ............... | 67 min | $V/R$ | 0.977 | 0.01 | 0.09 | |
| Hγ ............... | Orbital | $V/R$ | 0.978 | 0.10 | 0.05 | 0.65 |
| Hβ ............... | Orbital | $V/R$ | 0.981 | 0.08 | 0.05 | 0.69 |
| Hδ+Hγ+Hβ ... | Orbital | $V/R$ | 0.981 | 0.094 | 0.05 | 0.66 |

with the S wave model. Also apparent in Figure 6 is a systematic deviation of $V/R$ at a shorter period. Analysis of the residuals of $V/R$ from Figure 6, which are shown in Figure 7 folded on the shorter period, reveals a coherent variation accounting for 45% of the remaining variance at $P=0.02332\pm0.0003$ days, $T_o$ (time of maximum) $=2,444,322.512\pm0.001$ (ET) and half-amplitude of 0.052 with $\sigma_{SD}=0.04$. If the analyses of $V/R$ variation residuals are performed with and without inclusion of the 17 (out of 52) phase points within $\pm0.15\ \phi_o$ of eclipse (see Fig. 7), the following results for cosine fits are obtained: eclipse points excluded $T_o=2.512$, $P=0.02333$, half-amplitude $=0.053$, $\sigma_{SD}=0.03$; eclipse points only $T_o=2.514$, $P=0.02329$, half-amplitude $=0.052$, $\sigma_{SD}=0.04$. Thus, the 33.6 min period shows up clearly and consistently with the eclipse points excluded, or with only the points near eclipse included. This variation is at a period equal to $\frac{1}{2}P_h$ to within the errors. The combined coverage at Hδ, Hγ, and Hβ covers a total of 11 full cycles of the 33.6 minute period—without exception each of the 11 cycles shows points above and below the mean orbital cycle in a smooth, coherent fashion. The Hβ deviations even show a very slight lag of order 0.01–0.02 $\phi_o$ with respect to the Hδ and Hγ ratios obtained two nights earlier. This small lag two nights later would be expected due to the near, but not exact, commensurability of the orbital and 67 min variation ($44\times P_h$ is 0.001 day greater than $30\times P_o$), if the variation is at exactly $\frac{1}{2}P_h$. CHC noted a rapidly changing $V/R$ at $\phi_o=0.0$; we do not see this effect when allowance is made for the $\frac{1}{2}P_h$ cycle, although such an eclipse effect at $\phi_o=0.0$ would not be surprising. Although the $\frac{1}{2}P_h$ cycle is clearly present in the $V/R$ variations, we see no evidence for its existence in either the white light photometry or the equivalent width data.

In Figure 8 the equivalent widths of Hδ, Hγ, Hβ, and He II λ4686 are plotted against $\phi_o$ and $\phi_h$. The 67 min component accounts for fully 87% of the equivalent width variance in the Balmer lines and 48% of the He II 4686 variance (signal-to-noise ratio for the He II line is much lower than for the stronger Balmer lines). Clearly any periodic variations of either the equivalent widths or

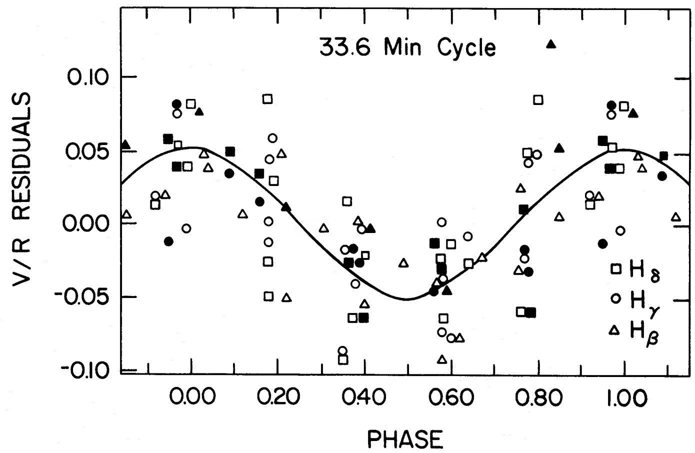


FIG. 7.—Residuals of $V/R$ after removing the smooth cosine function orbital variation for Hδ, Hγ, and Hβ. Phase is with respect to the 33.6 minute cycle. Solid line is best fit cosine curve. Solid symbols are from observations within 0.15 $\phi_o$ of eclipse.

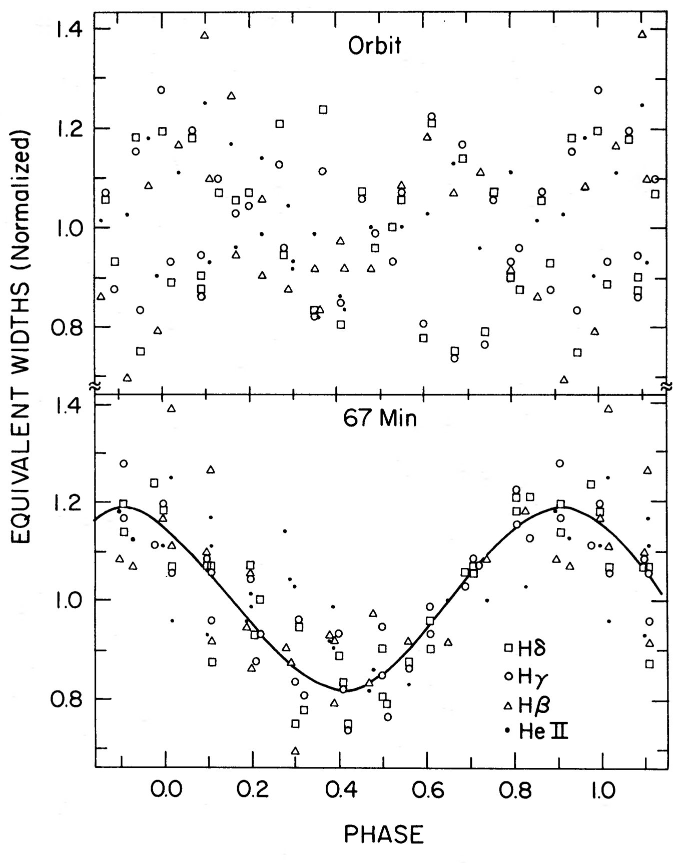


FIG. 8.—Equivalent widths vs. the orbital cycle for Hδ, Hγ, Hβ, and He II (equivalent widths normalized by 38.29, 53.56, 55.29, and 8.66, respectively, in both panels) are shown in the upper panel. The lower panel shows equivalent widths for Hδ, Hγ, Hβ, and He II with respect to the 67 min cycle; the solid line is the best fit cosine to the equivalent widths of the Balmer lines.

continuum fluxes (see § IV) are dominated by changes occurring at $\phi_h$. Phased cosine fits to the equivalent width data are summarized in Table 6. Since the equivalent widths peak less than or about $0.1 P_h$ earlier than the continuum fluxes, the line equivalent width variations actually represent line intensity variations of about a factor of 2, nearly in phase with and at a greater relative amplitude than the 67 min photometric variation.

We have examined the equivalent width residuals for periodicities after removing the dominant 67 minute variation. For both the Balmer lines and the He II λ4686 equivalent widths, time series analysis shows a small peak near 40 min as might be expected from an intermediate polar model with the white dwarf rotating at this period. The possible peak in the equivalent widths at ~40 min explains at most ~3% of the variance for the Balmer lines and ~8% for the He II line—the possible variation does not approach statistical significance. No evidence of equivalent width variations at either $\frac{1}{2}P_h$ or $\frac{1}{2}P_o$ was found.

## VI. RECONCILIATION WITH PREVIOUS RESULTS

We are in essentially complete agreement with the results of BV concerning spectroscopic behavior of EX Hya. Since the data set used here was obtained with higher temporal and spectral resolution than that of BV, but over as long a time base, we believe our results to be more precise.

However, we are in substantial disagreement with the more recent results of CHC. We suggest below several reasons for the discrepancies. Our spectral and temporal resolutions are comparable. CHC had superior spectral coverage, while we had more extensive and consistent temporal coverage. It should be kept in mind that EX Hya is a variable star. The possibility exists that between the observations of CHC in 1980 February and those discussed herein, obtained in 1980 March, the behavior of line intensities could have changed. This is not thought to be the most likely reason for the discrepancies and, of course, cannot explain differences in radial velocity amplitudes which can hardly have changed in this time.

CHC used data from three different nights to cover exactly one orbital cycle without any overlap of points with respect to $\phi_o$. EX Hya is known to be rather erratic from night to night. While the functional form of line intensity variations with respect to $\phi_o$ or $\phi_h$ is not likely to change from night to night, a slow drift of absolute intensity could occur from night to night making comparisons of partial cycles on different nights problematic. For the determination of $K_1$ small changes in line profiles or blending ratios could introduce systematic errors. The safest approach to measuring radial velocities is in a differential sense. One may reasonably expect, for instance, that the relative error of adjacent measures will have similar systematic errors, while measures separated in time are more likely to encounter systematic differences due to subtle changes in the star itself, the spectrograph, and the observing technique. In the CHC work a slight systematic error in absolute velocities between the first and second nights would directly introduce error into $K_1$ since all of the data points for phases 0.05 to 0.55 $\phi_o$ (radial velocity below the mean) were taken on the second night. Also, the use of different exposure times by about a factor of 3 on these different nights could be a source of systematic error (especially since CHC used a nonlinear image intensification system).

The adopted $K_1$ of CHC is based on a simultaneous fit to Hβ, Hγ, and Hδ data, although in their Figure 2 only one-half the scans are represented by points for Hδ and inclusion of this marginal line, which has the intrinsically largest scatter of all five lines measured, obviously increases $K_1$ *and* doubles the resulting error estimate. Adoption of the Hβ + Hγ solution with $K_1 = 80 \pm 14$ km s$^{-1}$ would seem a more reasonable choice. Furthermore, although 16 scans are cataloged in their Table 1, Hβ velocities are given for only 10 and Hγ for only 12 points, so that the CHC analysis uses unequal numbers and phase distributions of the different hydrogen lines. The different hydrogen lines have different $\gamma$ velocities. In the approach of BV of first averaging the velocities of separate lines any systematic absolute errors in the $\gamma$ velocities will cancel out to first order, while in the CHC analysis with unequal phase representations of different lines absolute errors in the $\gamma$ velocities will directly introduce errors in $K_1$.

As shown in Figure 2 our He II λ4686 velocities show the same variation as the Balmer lines, although the noise level is much increased. Thus we do not find the generally high positive velocities at phase 0.8–1.0 as reported by CHC. We do find high velocities at $\phi_o \approx 0.3$ —this is near the phase of minimum $V/R$ for the Balmer series. A change of line profile at $\phi_o \approx 0.3$ for He II is not apparent.

The different conclusions concerning the variation of line strengths versus $\phi_h$ can be explained as follows:

1) CHC obtained data over parts of a cycle over three nights with only partial coverage of the 67 min phase, thus making any interpretation problematic in an erratically variable star.

2) CHC state that equivalent width variations are unclear, but they do *not* see a minimum in equivalent widths at $\phi_h \sim 0.4$ as reported by BV. The $O - C$ for the 67 min cycle was at $-0.009$ days in early 1980 (see § IV). Thus the phase of the 67 min variation has not held from 1976 to 1980. The minimum at $\phi_h \sim 0.2$ in CHC corresponds to phase 0.4 in the corrected ephemeris. Allowing for the above, their minimum equivalent width timing is in complete agreement with the conclusions of BV and this paper.

Thus, for some of the differences between CHC as compared to BV and this paper, an unambiguous resolution is possible. The lack of adequate temporal coverage allowed CHC to reach an incorrect conclusion regarding line strength variations. Also their incorrect deduction from zero intensity line widths led to an incorrect result for the primary mass, given the other assumptions made. As to the $K_1 = 90 \pm 28$ km s$^{-1}$ derived by CHC it has a 1 $\sigma$ error which nearly includes both the results of BV and this paper in its range. Kraft (1964) set a probable upper limit of $K_1 = 50$ km s$^{-1}$ for EX Hya based on trailed coudé spectra. Given the more extensive and consistent data set studied in this paper and our agreement with BV, we feel confident in excluding the possibility (at the 95% confidence level) of $K_1 > 75$ km s$^{-1}$ for EX Hya.

## VII. MODELS FOR EX HYDRAE

Models which explain the 67 min variation in EX Hya have generally been variants of either modulated mass transfer from the secondary (VKS; Papaloizou and Pringle 1980), or a magnetized white dwarf rotating in such a way as to yield a 67 min variation (VKS; Warner and McGraw 1981).

Warner and McGraw (1981) have convincingly argued that the 67 min variation must be associated with nearly total modulation of the brightness of the hot spot component of EX Hya. Due to the large scatter of $O-C$ residuals and large changes of eclipse morphology, it is argued that the eclipses are best explained as grazing eclipses of the hot spot. Furthermore at times of total eclipses (flat bottomed profiles), the absolute minimum of eclipse depth is constant and independent of the phase with respect to the 67 min cycle. At maximum of the 67 min cycle the eclipse is quite deep, while at minimum the eclipse is very shallow. Warner and McGraw argue in favor of an intermediate polar model with radiation beamed from a white dwarf rotating at $\sim 40$ min. This period does not, however, show up in either the optical photometry (this paper) or hard X-rays (Heise 1981). We also examined the equivalent width data for possible periodicities at 40 min with ambiguous, but unconvincing results. The obvious signature of an intermediate polar is thus absent.

The period change derived in § IV is relevant to models for the 67 min variation. If the 67 min period is the result of beamed radiation at 40 min from a white dwarf, then the negative $P/\dot{P}$ derived in § IV implies that the central object is being spun up. Under the assumption that the central object is a white dwarf we can derive a lower limit to the required accretion rate by assuming that equatorial accretion at the surface Keplerian velocity is spinning up the white dwarf. By equating the angular momentum of the white dwarf and the angular momentum of the material accreted over a time scale $\tau_P$, the mass transfer rate required to spin up the white dwarf on a time scale $\tau_P$ may be shown to be

$$\dot{M} \sim \frac{\omega_{\rm WD}}{6.25\,\omega_{\rm acc}(M_{\rm WD})} \frac{M_{\rm WD}}{\tau_P} M_\odot \text{ yr}^{-1}, \qquad (1)$$

where the angular frequency of accreting material as a function of white dwarf mass, $\omega_{\rm acc}(M_{\rm WD})$, can be derived from the mass-radius relation of Shipman (1977). (The factor of 6.25 arises from adopting 0.4 as the radius of gyration for the white dwarf.) Numerically we find $\dot{M} \sim 2 \times 10^{-10}$ $M_\odot$ yr$^{-1}$ for a 0.8 $M_\odot$ white dwarf rotating at a period of 40 min. ($\dot{M}$ scales as $\sim M_{\rm WD}^{-0.5}$ for constant $\omega_{\rm WD}, \tau_P$.) Thus the period change does not demand an unreasonable accretion rate. If the central object is a magnetized white dwarf the accretion radius could be above the surface and magnetic coupling to slower moving material farther out may exist—both effects would require an upward revision of the above accretion rate.

If, however, the 67 min period arises from a modulation of the mass transfer rate (VKS; Papaloizou and Pringle 1979, 1980), then the period change represents the effect of changing secondary star or orbital eccentricity properties. Transfer of mass from $M_2$ to $M_1$ results in a shorter period excess for the proposed parametric instability due to an eccentric orbit (Papaloizou and Pringle 1979). Thus one might expect the binary system evolution to lead to a decreasing period as found in § IV. Papaloizou and Pringle (1980) estimate the time scale for the secondary remaining in resonance in EX Hya as $t_{\rm res} \sim \delta^n t_m$, where they suggest a canonical mass transfer time scale $t_m \sim 10^{8-9}$ yr and $\delta^n \gtrsim 0.01$. Thus $t_{\rm res} \sim 10^{6-7}$ yr, which brackets the time scale for the 67 min period change found in § IV. The coincidence of these two time scales is interesting, but it is not obvious that the time scales for period change and for existence of such a period need be the same. A more rigorous mathematical investigation of the proposed parametric instabilities would be necessary to adequately predict how the period should be changing.

The secondary cycle in the ratio of violet to red emission peak heights at $P \sim 33.6$ minutes must be explained by any successful model for the 67 min and orbital variations previously noted. We suggest the secondary $V/R$ variation is at $\frac{1}{2}P_h$ and not $\frac{1}{3}P_o$, although the current ability to discriminate between the two periods is at only the 1–2 $\sigma$ level of significance. Observations on three consecutive nights, with continuous coverage of about 1.5 orbital cycles each night, should be able to distinguish between the two possibilities. We do not see how the mass transfer instability as proposed by Papaloizou and Pringle (1980) can yield such a variation of $V/R$, although possible nonradial oscillations of the disk induced by a finite orbital eccentricity and modulated mass transfer should be investigated. We also do not see a specific explanation in terms of an intermediate polar model (Warner and McGraw 1981), although it is more difficult in this case to argue that such an explanation is unlikely. A simple 67 min modulation of the doubled emission with a superposed constant "S wave" does not explain the observations. A compound model with both modulated mass transfer (for $P_h$) and a white dwarf rotating at slightly greater than $\frac{1}{2}P_o$ (beat period of $\frac{1}{2}P_h$ and $P_o$) can explain the observations, but seems too contrived.

## VIII. CONCLUSIONS

We have presented observational results for EX Hya based upon simultaneous photometry and spectroscopy with good temporal and spectral resolution. Since the recent literature related to EX Hya has shown considerable disagreement, we are often at variance with some recent claims. Of particular note we have verified that the claims of BV concerning equivalent width variations with respect to the 67 min cycle are essentially correct, while the speculations of CHC concerning equivalent width variations are incorrect. This work supports the much lower orbital velocity amplitude found by BV, rather than the result of CHC; therefore we find that the primary mass is likely to be high (of order 1.4 $M_\odot$ as claimed by BV). We find clear spectroscopic evidence for the 67 min photometric period in the equivalent width variations of the Balmer lines where nearly 90% of the variance is so explained.

The photometric results yield conclusions significantly different from those claimed by VKS. We find no evidence for a changing orbital period and argue that the previous claim for such by VKS was not statistically significant. We do, however, find evidence for statistically significant shortening of the 67 min variation on a time scale of $2.8 \times 10^6$ yr.

A new periodicity at $\frac{1}{2}P_h$ is evidenced in the deviations of $V/R$ about the mean orbital variation for the Balmer emission peaks. Thus spectroscopic evidence also exists for a harmonic of the 67 min cycle. We failed to detect any evidence for a 40 min variation in either the white light photometry or spectroscopy, although a weak suggestion of such does appear in equivalent width variations.

We thank the staff of CTIO for providing competent and timely support of this study for which a new observing mode on the 4 m was encoded. Special thanks are in order to the CTIO night assistant Mr. Leonardo Alvay for enabling simultaneous photometry to be obtained. We thank Dr. B. Warner for discussion and Dr. A. Young for comments on the manuscript. This paper was initiated while the author enjoyed the stimulation of the Santa Cruz Workshop on Cataclysmic Variables and Related Systems.

## REFERENCES

Bateson, F. M. 1981, paper presented at the Santa Cruz Workshop on Cataclysmic Variables and Related Systems.
Bevington, P. R. 1969, *Data Reduction and Error Analysis for the Physical Sciences* (New York: McGraw-Hill).
Breysacher, J., and Vogt, N. 1980, *Astr. Ap.*, **87**, 349 (BV).
Córdova, F. A., and Riegler, G. R. 1979, *M.N.R.A.S.*, **188**, 103.
Cowley, A. P., Hutchings, J. B., and Crampton, D. 1981, *Ap. J.*, **246**, 489 (CHC).
Gilliland, R. L. 1982, *Ap. J.*, **254**, 653.
Heise, J. 1981, paper presented at the Santa Cruz Workshop on Cataclysmic Variables and Related Systems.
Kraft, R. P. 1964, *IAU Transactions*, Vol. **XIIB**, p. 519.
Kraft, R. P., and Krzeminski, W. 1962, in *Annual Report of the Director, Mount Wilson and Palomar Observatories*, 1961–1962, p. 20.
Mumford, G. S. 1967, *Ap. J. Suppl.*, **15**, 1.
Papaloizou, J., and Pringle, J. E. 1979, *M.N.R.A.S.*, **189**, 293.
______. 1980, *M.N.R.A.S.*, **190**, 13P.
Pringle, J. E. 1975, *M.N.R.A.S.*, **170**, 633.
Robinson, E. L. 1976, in *Ann. Rev. Astr. Ap.*, **14**, 119.
Shipman, H. L. 1977, *Ap. J.*, **213**, 138.
Vogt, N., Krzeminski, W., and Sterken, C. 1980, *Astr. Ap.*, **85**, 106 (VKS).
Warner, B. 1976, in *IAU Symposium 73, The Structure and Evolution of Close Binary Systems*, ed. P. Eggleton, S. Mitton, and J. Whelan (Dordrecht: Reidel), p. 85.
Warner, B. 1977, *Pub. Var. Star Sec. R.A.S. New Zealand*, **3**, 18.
Warner, B., and McGraw, J. T. 1981, *M.N.R.A.S.*, **196**, 59P.
Watson, M. G., Sherrington, M. R., and Jameson, R. F. 1978, *M.N.R.A.S.*, **184**, 79P.

RONALD L. GILLILAND: High Altitude Observatory/NCAR, P.O. Box 3000, Boulder, CO 80307